

# Effect of Excluded Volume and Anisotropy on Granular Statistics: ‘Fermi Statistics’ and Condensation

Daniel C. Hong

Physics, Lewis Laboratory, Lehigh University, Bethlehem, PA 18015, USA

**Abstract.** We explore the consequences of the excluded volume interaction of hard spheres at high densities and present a theory for excited granular materials. We first demonstrate that, in the presence of gravity, the granular density crosses over from Boltzmann to Fermi statistics, when temperature is decreased in the weak excitation limit. Comparisons of numerical simulations with our predictions concerning the scaling behavior of temperature with agitation frequency, gravity and particle-diameter show satisfying agreement. Next, within the framework of the Enskog theory of hard spheres, we interpret this crossover as a “condensation” of hard spheres from the dilute gas-state to a high density solid-like state. In the high density, low temperature limit Enskog theory fails because it predicts densities larger than the closed packed density below a certain temperature. We show how to extend the range of applicability of the Enskog theory to arbitrarily low temperatures by constructing a physical solution: all particles that are situated in regions with densities larger than a certain maximum density are assumed to be “condensed”.

## 1 Introduction

This paper is a review of a recently proposed theory of granular dynamics [1,2], which is based on the simple recognition that granular materials are basically a collection of hard spheres that interact with each other via a hard core potential [3]. For this reason, many of the properties of excited granular materials may be understood from the atomistic view of molecular gases, in particular from the point of view of kinetic theory [4]. There are, however, several distinctions between molecular gases and granular materials: First, the mean free path of the grains can be rather small – less than the particle diameter – even if the system is strongly forced. Second, granular material is made of macroscopic particles with finite diameter, and thus the material cannot be compressed indefinitely. When the mean free path vanishes, the density is the maximum, closed packed density. Third, gravity plays an important role in the collective response of granular materials to external stimuli because of the ordering of the particles according to their potential energy in the gravitational field.

For example, one of the notable characteristics of excited granular materials in a confined system under gravity is the appearance of a thin boundary layer near the surface that separates a fluidized region from a solid region.

This effect is also seen in shearing experiments [7], avalanches [8], and grains subjected to weak excitations [9,10]. In this limit, those grains in a solid region are effectively frozen, and thus do not participate in dynamical, diffusive processes. Hence, the conventional Boltzmann statistics, which is applicable in the limit of strong excitation and rapid flow where all the particles are dynamically active, certainly needs modification. Our first aim is to show that, in the weak excitation limit, the statistics where such a boundary layer appears, is analogous to the Fermi statistics. We will in fact demonstrate that the density profile of the grains is qualitatively well given by a Fermi function, from which we define the global temperature  $T$  and develop a thermodynamic theory of configurational statistics for excited granular materials. We present an explicit formula to relate the temperature  $T$  to the external control parameters such as the frequency  $\omega$  and amplitude  $A$  of the excitation vibration, the diameter  $D$  of the grains, and the gravitational acceleration  $g$ . Next, we examine the microscopic basis of the crossover from Boltzmann to Fermi statistics based on Enskog theory for hard spheres [11], and demonstrate how the crossover proceeds as grains condense from the bottom toward the surface.

## 2 Configurational Statistics and Maximum Entropy Principle: Justification of a Thermodynamic Approach

It is quite well known that variational methods are not useful in determining the properties of nonequilibrium systems. In systems that show e.g. periodic patterns, it is evident that one cannot perform variations about a steady state situation. Since the system being studied here is a dense, dissipative, nonequilibrium granular system, we find it necessary to make some comments on this point. If the mean free path of the grains is much less than a particle diameter, each particle may be considered to be effectively confined in a cage as also assumed for the free volume theory of dense liquids [12]. In such a case, the basic granular state is not a gas, but a solid or a crystal [1]. Thus an effective thermodynamic theory based on the free energy argument may be more appropriate than the kinetic theory. Our argument is that the dense state can be assumed as a “steady state” for which we compute the “configurational statistics” by means of the usual variational method as the most probable state.

To be more specific, consider the excitation of disordered granular materials confined in a box with vibrations of the bottom plate. The vibrations will inject energy into the system which cause the “ground state” to become unstable. A new, excited state will emerge with an expanded volume. The time average of such configurations which have undergone structural distortions, may be deviating weakly from the ground state so that the use of an

effective thermodynamic theory based on the variational principle could be justified.

Such a thermodynamic approach may be further justified by the following two recent experiments in both the weakly and the strongly excited regimes:

- *Weakly or moderately excited regime:* Clément and Rajchenbach (CR) [9] have performed an experiment with the vibrational strength, i.e. the dimensionless vibration acceleration  $\Gamma = A\omega^2/g$ , for a two dimensional vibrating bed, using inclined side walls to suppress convection. CR have found that the ensemble-averaged density profile as a function of height from the bottom layer obeys a universal function that is *independent* of the phase of oscillations of the vibrating plate. Namely, it is independent of the kinetics imposed on the system. One conceptually important point here is that the reference point of the density profile is not the bottom plate, but the bottom layer, which of course is fluidized.
- *Strongly excited regime:* Warr and Hansen (WH) [6] have performed an experiment on highly agitated, vertically vibrating beds of  $\Gamma \approx 30 - 50$  using steel balls with a large coefficient of restitution. They have found that the collective behavior of this vibrated granular medium *in a stationary nonequilibrium state* exhibits strong similarities to those of an atomistic fluid in *thermal equilibrium* at the corresponding particle packing fraction, in particular, concerning the two-point correlation function [6].

The results of both experiments indicate that for both moderately and strongly excited systems, a one-to-one correspondence seems to exist between the *configurational* statistics of the *nonequilibrium* stationary state and the *equilibrium* thermal state. In fact, this is not so surprising considering the fact that upon vibration, the granular materials expand and consequently the volume of the system increases. In turn, this increase corresponds to a rise in the potential energy after the configurational average is appropriately taken. Then the problem reduces to the packing problem, and the temperature-like variable,  $T$ , may be associated to the vibrating bed. The existence of distinctive configurational statistics in the density profile of CR (and also in WH in a special case) appears to be fairly convincing evidence that kinetic aspects of the excited granular materials may be separated out from the statistical configurations. These observations are the basis of the thermodynamic theory proposed in [1].

### 3 Fermi Statistics of Weakly Excited Granular Materials

We first view the system of granular particles as a mixture of holes and particles as in the lattice gas or the diffusing void model [12], which is the

simplest version of the free volume theory [13]. We now assign virtual lattice points by dividing the vibrating bed of width  $L$  and the height  $\mu D$ , with  $D$  typically the diameter of a grain and  $\mu$  the number of layers, into cells of size  $D \times D$ . Each row,  $i$ , is then associated with the potential energy  $\epsilon_i = mgz_i$  with  $z_i = (i - 1/2)D$  and  $m$  the mass of the grain. Note that the degeneracy,  $\Omega$ , of the each row is simply the number of available cells, i.e:  $\Omega = L/D$ . For a weakly excited system with  $\Gamma \simeq 1$ , the most probable configuration should be determined by the state that maximizes the entropy in the micro-canonical ensemble approach.

Taking into account the excluded volume effect which plays a similar role for dense granular systems as the Pauli principle in Fermi statistics, we derive the entropy  $S$ , defined as the total number of ways of distributing  $N$  particles into the system. Standard counting argument [14] yields,

$$S = \ln W = \ln \left( \prod_i \frac{\Omega!}{N_i!(\Omega - N_i)!} \right), \quad (1)$$

where  $N_i$  is the number of particles occupying the  $i$ -th row. Since gravity orders the grains with respect to their potential energy, a grain can be seen as a “spinless Fermion”, where the height  $z$  plays the role of the momentum variable (if one makes the connection to the electron gas). Maximizing  $S$  with the constraints,  $\sum_i N_i = N$  and  $\sum_i N_i \epsilon_i = \langle U(T(\Gamma)) \rangle$ , the mean steady state system energy, we find that the density profile,  $\phi(z)$ , which is the average number of occupied cells at a given energy level, is given by the Fermi distribution [1]:

$$\phi(z) = N_i/\Omega = 1/[1 + \exp(\beta(z - \mu))], \quad (2)$$

where  $\beta = mgD/T$ , the height is  $z = z_i/D$  and analogous to the Fermi energy,  $\mu$ , measured in units of  $D$ , is the number of layers in the low temperature limit, i.e. in the system at rest. Note that both  $\mu$  and  $T$  enter as Langrange multipliers introduced by the two constraints, i.e, the conserved number of particles and the mean energy. The global temperature  $T$  defined here is similar to the compactivity introduced by Edwards and his collaborators in their thermodynamic theory of grains [16], but is different from the kinetic temperature defined through the kinetic energy [17]. We point out that the Fermi statistics is essentially the macroscopic manifestation of the classical excluded volume effect and the anisotropy which causes the ordering of potential energy by gravity. In the spirit of the proposed analogy, the top surface of the granules at rest plays the role of the Fermi surface, and the grains in the thin boundary layer near the surface play the role of the excited electrons of a Fermi gas in metals.

For strongly excited systems, the exclusion principle does not apply. The Fermi analogy is valid when the zero temperature Fermi energy satisfies  $\mu \gg n_l$ , where  $n_l$  is the number of fluidized layers. Now, the energy  $E_i$ , injected

into the system is of the order of  $mA^2\omega^2/2$  and the potential energy  $E_p$ , needed to fluidize the particles in the top  $n_l$  layers is of the order of  $mg n_l D$ . Equating these two energies we find a necessary condition for the fluidization of the top  $n_l$  layers, namely:  $n_l \sim \Gamma A/(2D)$ . Hence, we expect the Fermi statistics to be valid for  $\Gamma \sim 1$ , if  $\mu \gg A/D$ .

#### 4 Relation between $T$ and $\Gamma$

We now relate the temperature  $T$  to the external control parameters such as  $\Gamma$ . First, a thermal expansion. We determine the energy per column  $\bar{u}(T) = \int_0^\infty \phi(z) m z g dz$ , from which we can determine the shift in the center of mass per particle;  $\bar{h}(T) = \bar{u}(T)/mg$ , which is given by:

$$\bar{h}(T) = h(0) \left[ 1 + \frac{\pi^2}{3} \left( \frac{T}{mgD\mu} \right)^2 \right] + \dots \quad (3)$$

with  $h(0) = D\mu^2/2$ . Second, a kinetic expansion. We make an observation that for a weakly excited granular system, most excitations occur near the Fermi surface, and thus the volume expansion may be effectively well represented by the maximum height,  $H_0(\Gamma)$  of a single particle bouncing on the vibrating plate assuming that the Fermi surface is in contact with the vibrating plate. The kinetic expansion,  $H_0(\Gamma)$ , is then determined by the maximum of  $\Delta(t)$  in the following equation that describes the trajectory of a single ball on a vibrating plane with intensity  $\Gamma = \omega^2/g$  with  $A$  the amplitude,  $\omega$  the frequency of the vibrating plate, and  $g$  the gravitational constant:

$$\Delta(t) = \Gamma(\sin(t_0) - \sin(t)) + \Gamma \cos(t_0)(t - t_0) - \frac{1}{2}(t - t_0)^2 \quad (4)$$

in units of  $g = \omega = 1$ , where  $t_0 = \sin^{-1}(1/\Gamma)$ . Note that since  $\Delta$  is the relative distance between the ball and the plate, it cannot be negative. More precisely, the particle is launched from the plate at  $t = t_0$  by inertia, and then makes a free flight motion until it strikes the plate. It then stays on the plate until  $t = t_0 + 2\pi$ , when it is launched again and repeats the same motion. Hence,  $\Delta$  is a periodic function with period  $2\pi$ . Since the Fermi distribution near  $T = 0$  can be approximated by a piecewise linear function and  $H_0(\Gamma)$  is thought to be the edge of the function, we expect  $H_0(\Gamma) \approx \Delta h/2 = (\bar{h}(T) - h(0))/2$ . By equating the thermal expansion, (3), to the kinetic expansion,  $H_0(\Gamma)g/\omega^2$ , in physical units, we now complete our thermodynamic formulation by presenting the explicit relation between  $T$  and  $\Gamma$  [1]:

$$T = \frac{mg}{\pi} \left( 3D \frac{gH_0(\Gamma)}{\omega^2} \right)^{1/2}. \quad (5)$$

In MD simulation, one may measure the maximum height,  $\bar{h}_o(\Gamma)$ , of a single ball on a vibrating plate and replace  $gH_0(\Gamma)/\omega^2$  with  $2\bar{h}_o(\Gamma)/\alpha$  with  $\alpha$  an adjustable parameter [15].

Now we compare our theoretical prediction with an experimental result of Clément and Rajchenbach [9]. Figure 1 shows the fitting of the experimental density profile for  $\Gamma = 4$  of CR by the scaled Fermi distribution,  $\phi(z) = \rho(z)/\rho_c$ , with  $\rho_c$  the closed packed density. For hexagonal packing,  $\rho_c \approx 0.92$ . The fitting value of  $T/mg$  is 2.0 mm, while Eq.(5) yields  $T/mg \approx 2.6$  mm. The agreement between the two is fairly good in spite of such a simple calculation. This expression also agrees with the simulation result [10,15].

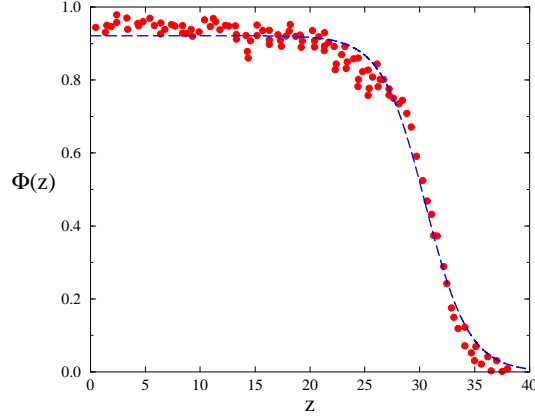


**Fig. 1.** Density  $\phi(z)$  as a function of the height  $z$ . The symbols are the data by Clément and Rajchenbach and the dotted line is the Fermi distribution function, Eq.(2).

Note that the detailed expression of  $H_0(\Gamma)$  depends on the manner by which the grains are excited and we expect that our main scaling prediction of Eq.(5), namely  $T \propto g^{3/2}D^{1/2}/\omega$ , will hold even for systems driven not by sinusoidal waves. Further,  $T$  has a gap at  $T = 0$  because the time between the launching and landing of the ball is always finite for  $\Gamma > 1$ . Next, it is well known that the *specific heat* per particle,  $C_v = d\bar{u}/dT$ , can be written as the fluctuations in the energy, namely  $\langle(\Delta\bar{u})^2\rangle = \langle(\bar{u}(z) - \bar{u})^2\rangle = T^2C_v$  [18]. Hence, our theory makes a nontrivial prediction for the fluctuations in the center of mass:

$$\langle(\Delta z)^2\rangle = \langle(z(T) - \langle z \rangle)^2\rangle = \frac{\langle(\Delta h)^2\rangle}{\mu_o^2} = \frac{\pi^2}{3} \left( \frac{T}{mgD} \right)^3 \frac{D^2}{\mu_o^2} \quad (6)$$

while the center of mass is given by:

$$\Delta z(T) = z(T) - z(0) = \frac{D\mu_o\pi^2}{6} \left( \frac{T}{mgD\mu_o} \right)^2 \quad (7)$$

Note that the total expansion,  $\Delta h(T) \equiv \mu_o \Delta z$  and its fluctuations  $\langle(\Delta h)^2\rangle/D^2 = \langle\mu_o(\Delta z)^2/D^2\rangle$  are only a function of the dimensionless Fermi temperature

$T_f = T/mgD$  as expected. Furthermore, note that (6) is an indirect confirmation that the specific heat is linear in  $T$  as it is for the non-interacting Fermi gas.

## 5 Test of Fermi Statistics by Molecular Dynamics Simulations

In this section, we examine the configurational statistics of granular materials in a vibrating bed, in particular the density profile, and its fluctuations by MD simulations and compare the results with the predictions made in the previous chapter. The MD code was provided by the authors of [19] and the details of the code can be found in the literature. Simulations were carried out in two dimensional boxes with vertical walls for  $N$  particles each with a diameter  $D = 0.2$  cm and a mass  $m = 4\pi(D/2)^3/3$  with the degeneracy  $\Omega$  using  $(N, \Omega) = (100, 4), (200, 4)$  and  $(200, 8)$  with a sine wave vibration. The dimensionless Fermi energy  $\mu = N/\Omega$  is the system height at rest. For all cases, the inequality  $\mu \gg A/D$  was satisfied. In Fig. 2 the temperature, obtained by the best fit of the density profile to the Fermi function (dots), is plotted against  $\Gamma$  and the values predicted by Eq.(5). Note the fairly good agreement between theory and simulations.

We also studied the temperature scaling against the frequency, gravity and diameter to further check the validity of Eq. (5). The scaling laws as determined by the simulations are:

$$T \approx \omega^{-m_1}$$

$$T \approx g^{m_2}$$

$$T \approx D^{m_3}$$

with  $m_1 \approx 1.16$ ,  $m_2 \approx 0.48$ , and  $m_3 \approx 0.53$ . These values are close to the predicted ones by Eq. (5), i.e  $m_1 = 1$ ,  $m_2 = 0.5$ ,  $m_3 = 0.5$ . For detailed comparisons, see the original paper [15].

Finally, we have also checked the scaling of the center of mass, and the fluctuations against  $T^2$  and  $T^3$ . Since the density profiles are well fitted by the Fermi function, we anticipate that the center of mass and its fluctuations obey the scaling as shown in Figs. 3 and 4. Note that the increase in the center of mass is *second* order in temperature  $T$ , which is contrary to the mean field prediction of the linear increase of volume in the compactivity  $X$  [16].

## 6 Condensation of Hard Spheres Under Gravity

Our next goal is to examine the microscopic basis of Fermi statistics based on the kinetic theory, in particular the Enskog equation for hard spheres of

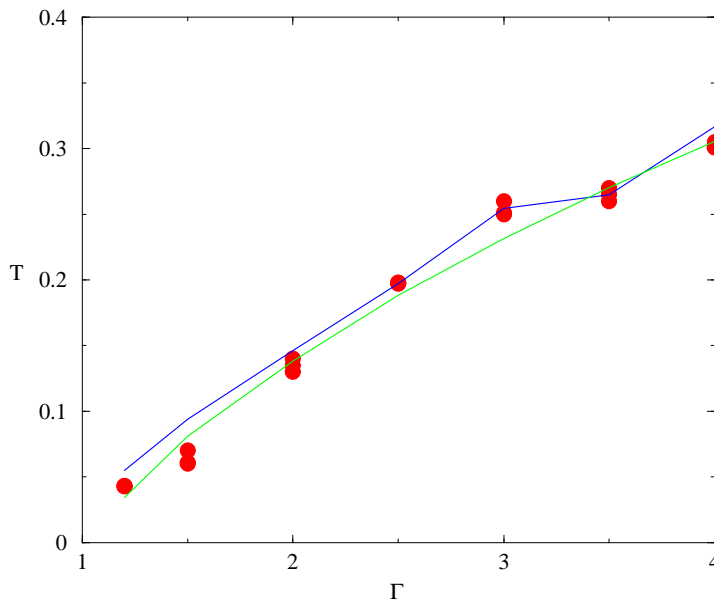


**Fig. 2.** Comparison between the measured temperatures by MD(dots) and the predicted ones. The lower line was obtained by Eq.(5), while the upper one was obtained by replacing  $gH_o/\omega^2$  by  $2\bar{h}_o(\Gamma)/\alpha$  with  $\alpha \approx 12.8$ .  $\bar{h}_o(\Gamma)$  is the maximum jump height of a single ball on a vibrating plated obtained by MD.

mass  $m$  and diameter  $D$ , to explore whether or not the kinetic theory can describe the cross over from Boltzmann to Fermi statistics and if so, under what conditions it occurs.

Our particularly interesting discovery [2] is that the prediction of the Enskog equation is only valid when  $\beta\mu \leq \mu_o$ , where  $\mu$  is the dimensionless initial layer thickness of the granules (or the Fermi energy),  $\beta = mgD/T$  with  $T$  the temperature, and the critical value,  $\mu_o$ , is determined to be  $\mu_o = 21.756$  in two dimensions (2D) and  $\mu_o = 15.299$  in three dimensions (3D). (For maximum packing,  $\mu_o = 151.36$  in 3D and  $\mu_o = 144.6155$  in 2D.) When this inequality is violated, the Enskog equation does not conserve the particles, and we present a scenario of resolving this puzzle based on physical intuition, namely that the missing particles condense from the bottom toward the surface [2]. In this way, the hard sphere Enskog gas appears to contain the essence of Fermi statistics. We briefly describe how the density profile,  $\phi$  as a function of dimensionless variable  $\zeta$ , can be obtained from the Enskog equation. For details, see Ref. [2]. Note that  $\phi$  introduced here is not the volume fraction  $\nu$  but is scaled so that  $\phi = 1$  at closed packing.

In a free volume theory, particles are confined in a cage. Hence, if we use a simple cubic lattice as a basic lattice, the close packed volume fraction  $\rho_c = N/V = N/(D^2N) = 1/D^2$ . If we define the dimensionless density



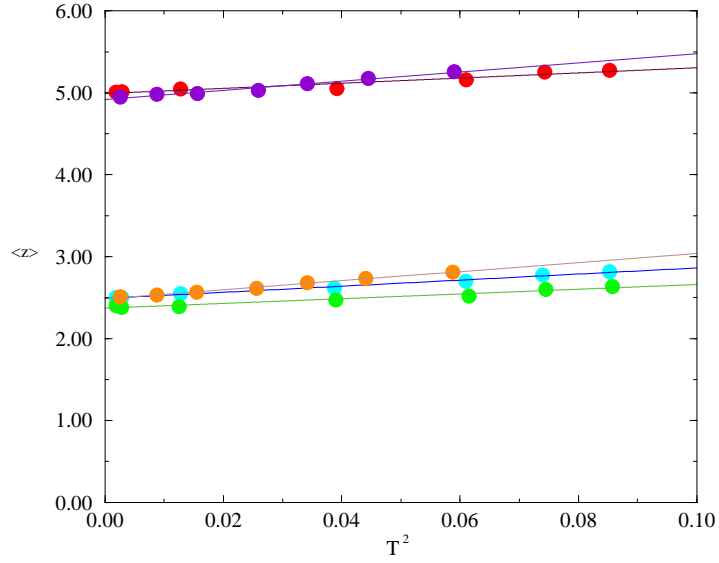


**Fig. 3.** Center of mass as a function of temperature. The upper ones are data for sine wave and triangular wave excitations with  $(N, \Omega) = (200, 4)$  for different  $\Gamma$ 's. The lower ones are the same with  $(N, \Omega) = (100, 4)$ .

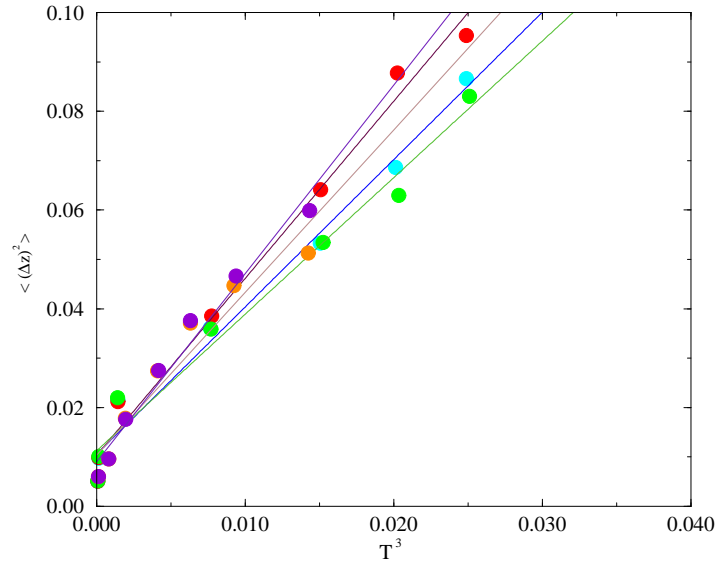


**Fig. 4.** Fluctuations in the center of mass as a function of temperature. Symbols used are the same as in Fig. 3.

$\phi(z) = G(z)/\rho_c = D^2G(z)$  or  $\phi(\zeta, \beta) = D^2G(z)$  with  $\zeta = z/D$ , we then obtain the following exact dimensionless equation of motion for  $\phi(\zeta, \beta)$ :

$$\frac{d\phi(\zeta)}{d\zeta} + \beta\phi(\zeta) = \phi(\zeta)I_\zeta(\zeta) \quad (8)$$

where  $\beta = mgD/T$  and

$$I_\zeta(\zeta) = \frac{1}{2} \int_0^{2\pi} d\theta \cos \theta [\chi(\zeta - \frac{1}{2} \cos \theta) \phi(\zeta - \cos \theta) - \chi(\zeta + \frac{1}{2} \cos \theta) \phi(\zeta + \cos \theta)] \quad (9)$$

For 3D, the corresponding equation for the density  $\phi(\zeta) = D^3G(z)$  is given by Eq.(8) with:

$$I_\zeta(\zeta) = \pi \int_0^\pi d\theta \sin \theta \cos \theta [\chi(\zeta - \cos \theta/2) \phi(\zeta - \cos \theta) - \chi(\zeta + \cos \theta/2) \phi(\zeta + \cos \theta)] \quad (10)$$

Several forms for the equilibrium correlation function  $\chi$  have been proposed, but we use the following widely used forms: For 2D, we use the form proposed by Ree and Hoover [20]:  $\chi(\phi) = (1 - \alpha_1\phi + \alpha_2\phi^2)/((1 - \alpha\phi)^2)$  with  $\alpha = 0.489351 \bullet \pi/2 \approx 0.76867$ ,  $\alpha_1 = 0.196703 \bullet \pi/2 \approx 0.30898$ ,  $\alpha_2 = 0.006519 \bullet \pi^2/4 \approx 0.0168084$ , while for 3D, we use the form suggested by Carnahan and Starling [21]:  $\chi(\phi) = (1 - \pi\phi/12)/(1 - \pi\phi/6)^3$

Since the total number of particles,  $N$ , remains fixed, the following normalization condition should be satisfied for both 2D and 3D.

$$\int_0^\infty d\zeta \phi(\zeta; \beta) = \mu \quad (11)$$

where  $\mu \equiv N/\Omega_x$  (or  $\mu \equiv N/\Omega_x\Omega_y$  in 3D) is the Fermi energy and  $\Omega_x, \Omega_y$  are the degeneracies along the x and y axes. We now perform the gradient expansion of (9) and (10) and retain only the terms to first order in  $d\chi/d\zeta$ . The 3D solutions for the first order differential equation can be obtained easily, and are given by [2]:

$$-\beta(\zeta - \bar{\mu}) = \ln \phi - 1/(1 - \alpha\phi)^2 + 2/(1 - \alpha\phi)^3 \quad (12)$$

$$\beta\bar{\mu} = \ln(\phi_o) - 1/(1 - \alpha\phi_o)^2 + 2/(1 - \alpha\phi_o)^3 \quad (13)$$

$$\beta\mu = \phi_o - \frac{2\phi_o}{1 - \alpha\phi_o} + \frac{2\phi_o}{(1 - \alpha\phi_o)^3} \quad (14)$$

where  $\alpha = \pi/6$ . For given values of  $\beta$  and  $\mu$ ,  $\phi_o \equiv \phi(\zeta = 0)$  will be determined by Eq.(14) with the condition that  $\phi_o$  cannot in anyway greater than the closed packed density. As we will see, we need care to proceed. First, since

the right hand side of (14) is an monotonically increasing function of  $\phi_o$  and  $\phi_o$  cannot be greater than the closed packed density, which is 1 in our units,  $\beta\mu$  must have an upper bound  $\mu_o$ ; namely,  $\mu_o = 15.299$  in 3D, ( $\mu_o = 21.756$  in 2D), which is the value obtained by setting  $\phi_o = 1$  in the right hand side of (14). Note that this upper limit depends on the underlying basic lattice structure. (For a hard sphere gas in a continuum space, at the closed packed density,  $\eta = \frac{4\pi}{3}(\frac{D}{2})^3 = \frac{\pi}{6}\phi \approx 0.74$  in 3D and  $\eta = \frac{\pi}{4}\phi = \pi/2\sqrt{3} \approx 0.907$  in 2D hexagonal packing, in which case, the upper limit  $\mu_o = 151.36$  in 3D and  $\mu_o = 144.6155$  in 2D.) Considering the fact that both the temperature  $T$  and the Fermi energy  $\mu$  are *arbitrary* control parameters, the existence of such bounds is a puzzle: if  $\beta\mu$  is less than  $\mu_o$ , then the density profile given by Eq.(12) is well defined, but if  $\beta\mu$  is greater than  $\mu_o$ , then  $\phi_o$  must be one at the bottom, and the particle conservation appears to break down, namely

$$\int_o^1 d\zeta\phi(\phi) = \int_0^\infty d\zeta\phi(\zeta) \equiv \mu_o/\beta < \mu \quad (15)$$

The central question is: where does the rest of the particles go? In order to gain some insight into this question, consider first the case of point particles under gravity, in which case the density profile is given by:  $\rho(\zeta) = \rho(0)\exp(-mg\zeta/T)$ . If we put more particles into the system, we simply need to increase  $\rho(0)$  because the point particles can be compressed indefinitely, and the profile simply shifts to the right. We now replace these point particles with hard spheres, which cannot be compressed indefinitely and thus the maximum density at any point is the closed packed density. Suppose we have a system of hard spheres at a certain temperature  $T$ , where the density is closed packed at the bottom layer and smoothly decreases toward the surface. At this point, if we add more hard spheres, say the amount of one layer, to the system, how does the density profile modify? Since the hard spheres cannot be compressed, our intuition tells us that after the system reaches the equilibrium, the density of the first(bottom) and second layer becomes closed packed, forming a rectangle, which is then followed by the original Enskog profile. If we keep adding more particles, we obtain the density profile that is the combination of the rectangle (we term this the Fermi rectangle) beginning at the bottom and the smooth original Enskog profile, which adjoins the Fermi rectangle at its upper edge. The total number of hard spheres in the Fermi rectangle should be the same as that of the added particles. One may obtain the same picture in a reverse way. Suppose we start from a high temperature where all the particles are active. We then slowly decrease the temperature to suppress the thermal motion. There will be a temperature where the density at the bottom is the closed packed density. Now, let us lower the temperature further. What happens? The next layer will become closed packed and is thus effectively frozen. As we keep lowering the temperature, the freezing of the particles will occur from the bottom and the frozen region will then spread out, until at  $T=0$  all the particles are frozen.

Note that the frozen particles in the closed packed region behave like a solid with  $\phi_o = 1$ . Such an observation helps us to resolve the puzzle associated with the disappearance of particles. The missing particles should form the condensate in the Fermi rectangle spanning the bottom to the lower part of the fluidized layer. We term the surface that separates the frozen or a closed packed region with  $\phi = 1$  from the fluidized region with  $\phi < 1$  the Fermi surface. The location of the Fermi surface,  $\zeta_F$ , is determined by the number of the missing particles, namely,  $\zeta_F = \mu - \mu_o/\beta$ , and is thus a function of temperature. For nonzero  $\zeta_F$ , we must put the missing particles below the Fermi surface and shift the bottom layer from  $\zeta = 0$  to  $\zeta_F$ . From Eq.(15), we find that in 2D the number of missing or condensed particles,  $N_o(T)$ , at  $T < T_c$  is  $N_o(T) = \Omega_x(\mu - \mu_o/\beta) = N(1 - T/T_c)$ , where  $N(\equiv \Omega_x\mu)$  is the total number of particles, and  $T_c$  is the condensation temperature defined as the point where the particle conservation, Eq.(15), breaks down, namely

$$T_c = mgD\mu/\mu_o \quad (16)$$

Hence, the fraction of condensed particles is given by:

$$N_o(T)/N = 1 - T/T_c \quad (17)$$

How is this picture modified in the presence of dissipation? With dissipation, solving the Enskog equation becomes a nontrivial task for three reasons: First, we do not yet know the precise functional form of the velocity distribution function for inelastic particles. Experimentally observed profiles [23] definitely indicate that they are not Gaussian. Second, even if we somehow have empirical formulas for the velocity distribution functions, carrying out the integral with non-Gaussian profiles for the Enskog integro differential operator becomes a non-trivial task. Third, in the presence of dissipation, the temperature profile is nonuniform [24], and thus one has to solve the equation for the density profile, i.e., Eq.(8), along with the energy equation [25]. Analytic solution for this case is difficult to obtain. However, if the dissipation is small, then one might assume that the velocity distribution function is still Gaussian and the temperature remains uniform except near the heat reservoir. Under such assumption, we only need to solve the Eqs.(8)-(10) with the corrected pressure term [4], which is given by:

$$P = \rho T[1 + \gamma \rho D^d \chi]$$

where  $\gamma = \frac{\pi}{4}(1 + \epsilon)$  when  $d = 2$  and  $\gamma = \frac{\pi}{3}(1 + \epsilon)$  when  $d = 3$ . Since the solution of the force balance equation,  $dP/dz = -\rho g$  yields the same result, in the presence of dissipation, we use the force balance equation instead of solving the Enskog equation as was done in the elastic case [2]. eDefining  $\phi = \rho D^d$  as above and using the above forms of  $P$  in the force balance equation yields the differential equation

$$\beta\phi(\zeta) + d\phi(\zeta)/d\zeta = -\gamma[\phi d\chi(\phi)/d\phi + 2\chi(\phi)d\phi(\zeta)/d\zeta] \quad (18)$$

Upon integration we find in the two dimensional case:

$$\beta(\zeta - \bar{\mu}) = -\log \phi + c_1 \phi + c_2 \log(1 - \alpha\phi) + c_3/(1 - \alpha\phi) + c_4/(1 - \alpha\phi)^2 \quad (19)$$

where

$$\begin{aligned} c_1 &= -2\gamma\alpha_2/\alpha^2, \\ c_2 &= \gamma(\alpha_1/\alpha^2 - 2\alpha_2/\alpha^3) \\ c_3 &= -c_2 \\ c_4 &= \gamma(-1/\alpha + \alpha_1/\alpha^2 - \alpha_2/\alpha^3) \end{aligned}$$

Then  $\beta\bar{\mu}$  is the negative of the right hand side of (19) with  $\phi$  replaced with  $\phi_0 \equiv \phi(\zeta = 0)$ . Integrating  $\beta\zeta$  from zero to  $\phi_0$  yields

$$\beta\mu = c_5 + c_6\phi_0 - c_2\phi_0^2 + c_7/(1 - \alpha\phi_0) + c_8/(1 - \alpha\phi_0)^2 \quad (20)$$

where

$$\begin{aligned} c_5 &= \gamma(-2\alpha_1\alpha + \alpha^2 + 3\alpha_2)/\alpha^4 \\ c_6 &= -c_2 + 1 \\ c_7 &= -\gamma(2\alpha^2 - 3\alpha_1\alpha + 4\alpha_2)/\alpha^4 \\ c_8 &= -c_4/\alpha \end{aligned}$$

This result may be shown to be equivalent to the elastic case when  $\epsilon = 1$ . Substituting the numeric values for the constants  $\alpha$ ,  $\alpha_1$ ,  $\alpha_2$  and evaluating at  $\phi_0 = 1$  yields

$$\mu_0 = 1 + 10.3779(\epsilon + 1) \quad (21)$$

In three dimensions we find

$$\beta(\zeta - \bar{\mu}) = -\log \phi - \frac{1}{4} \frac{\gamma}{\alpha(1 - \alpha\phi)^2} - \frac{1}{2} \frac{\gamma}{\alpha(1 - \alpha\phi)^3} \quad (22)$$

where  $\beta\bar{\mu}$  is again given by the negative of the right hand side of (22) with  $\phi_0$  replacing  $\phi$ . Then we integrate  $\beta\zeta$  between zero and  $\phi_0$  to get

$$\beta\mu = \phi_0 + \frac{1}{2} \frac{\gamma\phi_0^2}{(1 - \alpha\phi_0)^2} + \frac{1}{2} \frac{\gamma\phi_0^2}{(1 - \alpha\phi_0)^3} \quad (23)$$

where  $\alpha = \pi/6$ . When  $\epsilon = 1$ , this again reduces to the profile for the elastic hard spheres (12). We find upon evaluating  $\beta\mu$  at  $\phi_0 = 1$  that

$$\mu_0 = 1 + 7.14964(\epsilon + 1) \quad (24)$$

We note that in general,  $\mu_0$  takes the form  $1 + C(\epsilon + 1)$ , and we recall that  $T_c = mgD\mu/\mu_0$ . Hence we may write

$$T_c(\epsilon) = T_c(\epsilon = 1) + \frac{mgD\mu C(1 - \epsilon)}{(1 + 2C)(1 + C(\epsilon + 1))} \quad (25)$$

Letting  $\delta = (1 - \epsilon) \ll 1$ , we may recast the above result as

$$T_c(\epsilon) = T_c(\epsilon = 1) + \frac{mgD\mu C}{(1 + 2C)^2}\delta + \frac{mgD\mu C^2}{(1 + 2C)^3}\delta^2 + \dots \quad (26)$$

In summary, we conclude that the condensation phenomenon persists in the presence weak of dissipation. Note that in the above analysis, we set  $\phi_o = 1$  as the upper bound for a cage model. For maximum packing,  $\phi_o$  can exceed unity, as discussed before, i.(in 3D,  $\phi_o \approx 0.74 \pi/6$  and  $\phi_o = 2/\sqrt{3}$ .) The clustering of particles near the bottom wall in two dimensional experiments [27] may be a strong confirmation of this scenario.

## 7 Conclusion

In this review, we have explored simple consequences of excluded volume interaction for dense granular materials, and shown that the granular statistics cross over from Boltzmann to Fermi statistics as the strength of the excitation is reduced. We have also advanced a theory that such a crossover may be understood as the condensation of hard spheres below a condensation temperature. Since the Enskog equation breaks down at high densities, comparable to the closed packed density, we have constructed physical solutions beyond this regime by forming the Fermi rectangle near the bottom. Those particles in the Fermi rectangle are assumed to be condensed. This way, we have extended the applicability of the Enskog theory to arbitrarily low temperatures.

As demonstrated in Eq.(14), the Enskog solution based on a virial expansion from the dilute to the dense case conserves particles only when we allow the density profile greater than the maximum closed packed density at the bottom, which is clearly unphysical. This is due to the fact that the equation of state, i.e. the pressure as function of density, is not known for all densities. If one would use the correct equation for the pressure (which is not analytically known at this point, except for a numerically determined one [29]) that must *diverge* at the close packed density, it may be possible that the strange condensation phenomenon associated with the Enskog equation may be absorbed by an advanced theory [29]. We point out, however, that even with this empirical pressure profile the formation of Fermi rectangle is clearly visible. [29] The density profile above the Fermi rectangle was shown to be nicely fit by the Enskog profile. Thus, our picture of condensation, which is an alternative way to extend Enskog theory results up to the maximum possible density, seems to capture the essence of physics – and we have shown analogies to the Fermi statistics.

For a polydisperse system, the upper limit for  $\eta$  is usually larger than that of the monodisperse system. Thus, we expect the freezing temperature to be much lower for a polydisperse system. Note, however, that as long as the upper limit for  $\eta$  is smaller than unity, Enskog theory for a gas predicts the condensation phenomenon, in the sense that unphysical densities are predicted. For the extreme limit of an Appolonian packing [28], for which the close packed density can be unity,  $\eta = \alpha\phi_o$  in (14) can be arbitrarily close to unity and thus the right hand side of (14) can be arbitrarily large. In this case, the condensation phenomenon discussed in this paper disappears.

The original experiment done in Ref. [9] used a rectangular box with tilted side walls, but one may use a different shape such as a parabola to mimic the density profile of the electron gas in 3D, which may help one to visualize the excitation spectrum near the Fermi surface. Finally, we point out that while it is trivial to drive hard sphere grains by a thermal reservoir in MD simulations, it becomes a nontrivial task to do this experimentally. The normal way of exciting the granular system experimentally is through vibration, yet it remains an unresolved issue to determine the precise relation between the vibration strength and the effective temperature of the reservoir. Eq.(5), which is based on a single ball picture, may be a first step in this direction. The discovery of the Fermi statistics and the associated condensation phenomena may provide an avenue to apply the methods developed in equilibrium statistical mechanics to the study of granular dynamics, notably from the point of view of elementary excitations such as the Fermi liquid theory in condensed matter physics.

## Acknowledgments

I wish to thank H. Hayakawa for collaboration and J. A. McLennan for helpful discussions on the Enskog equation. I also wish to thank Paul Quinn for carrying out MD simulations and Joseph Both for checking some of the algebra in section 6, as well as S. Luding for discussions on the Appolonian packing and the puzzle associated with the condensation phenomenon.

## References

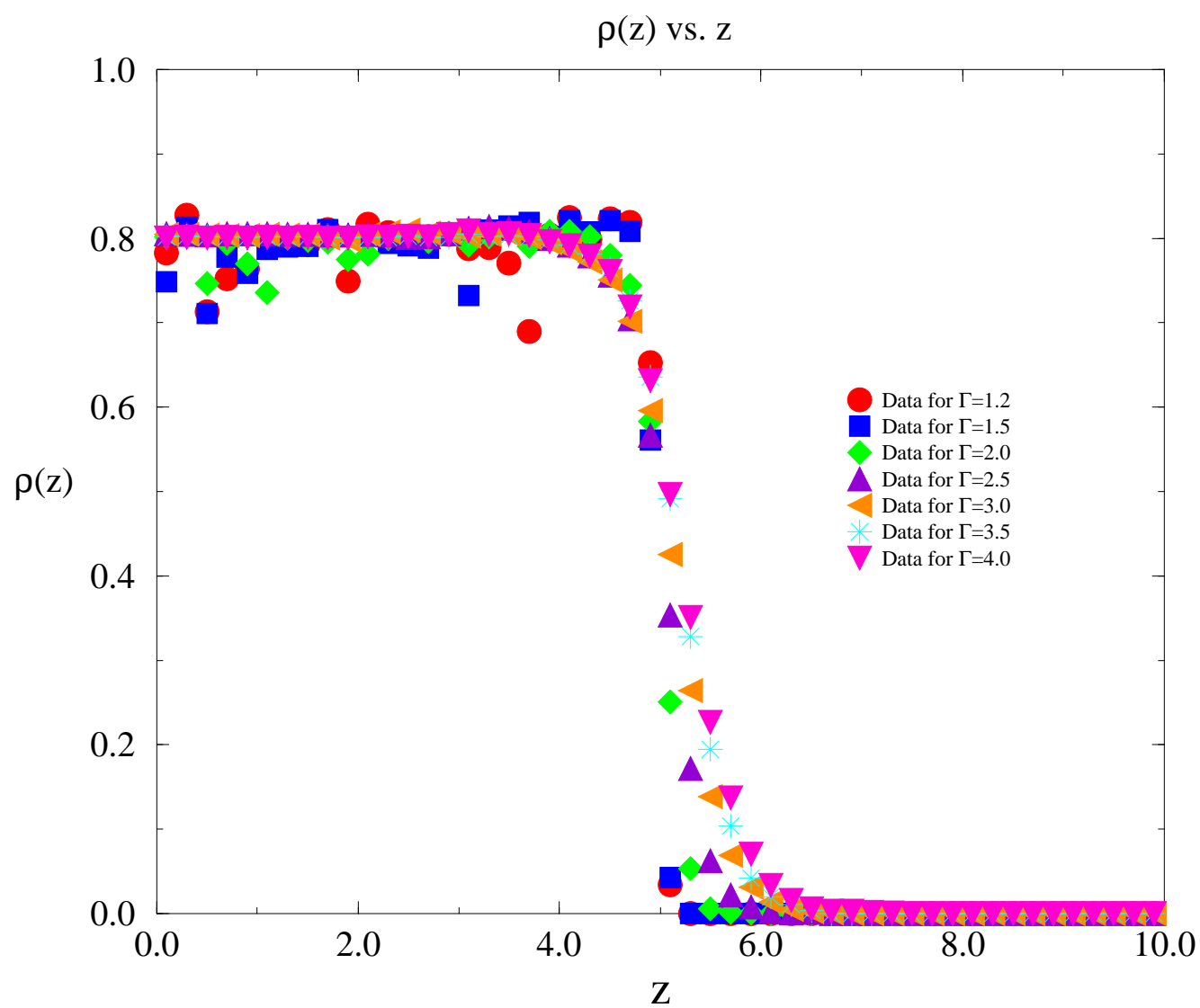
1. H. Hayakawa and D. C. Hong, Phys. Rev. Lett., **78**, 2764 (1997).
2. D. C. Hong, cond-matt/9806253 (to appear in Physica A, 1999).
3. H. Jaeger, S. R. Nagel and R. P. Behringer, Physics Today, **49**, 32 (1996), Rev. Mod. Phys. **68**, 1259 (1996); H. Hayakawa, H. Nishimori, S. Sasa and Y-h. Taguchi, Jpn. J. Appl. Phys. Part 1, **34**, 397 (1995) and references therein.
4. J. Jenkins and S. Savage, J. Fluid. Mech. **130**, 197 (1983); S. Chapman and T. G. Cowling, *The Mathematical Theory of Nonuniform Gases* (Cambridge, London, 1970); J. A. McLennan, *Introduction to Non-Equilibrium Statistical Mechanics*, Prentice Hall (1989).

5. This is similar to the case of electron gas subjected to thermal excitation, in which case only electrons near the Fermi surface are excited. Note that while the exclusion principle operates in momentum space for an electron gas, for grains, the corresponding exclusion principle operates in real space.
6. S. Warr and J. P. Hansen, Europhys. Lett. Vol. 36, no.8 (1996). Urbach also found that the two point correlation function of excited granular system is the same as that of the equilibrium hard sphere gas at the equivalent packing density (See his paper in this book.)
7. D. M. Hanes and D. Inman, J. Fluid. Mech. **150**, 357 (1985); S. Savage and D. Jeffrey, *ibid*, **110**, 255 (1981).
8. For example, see: J. P. Bouchaoud, M. E. Cates, R. Prakash, and S. F. Edwards, J. Phys. France **4**, 1383 (1994).
9. E. Clément & J. Rajchenbach, Europhys. Lett. **16**, 133 (1991).
10. J. A. C. Gallas, H. J. Herrmann & S. Sokolowski, Physica A **189**, 437 (1993).
11. D. Enskog, K. Sven. Vetenskapsakad. Handl. **63**, 4 (1922).
12. H. Caram & D. C. Hong, Phys. Rev. Lett., **67**, 828 (1991); Mod. Phys. Lett. B **6**, 761 (1992); For earlier development, see J. Litwinyshyn, Bull. Acad. Polon. Sci., Ser. Sci. Tech. **11**, 61 (1963); W. W. Mullins, J. Appl. Phys. **43**, 665 (1972).
13. T. L. Hill, *Statistical Mechanics*, Chap.8, New York, Dover (1985).
14. For example, see Eq.8.41 in Huang, Statistical Mechanics, Second Edition, Wiley (1987).
15. P. Quinn and D. C. Hong, cond-matt/9901113 (To appear in Physica A, 1999).
16. S.F. Edwards and R.B.S. Oakeshott, Physica A **157**, 1080 (1989); A. Mehta and S.F. Edwards, Physica A(Amsterdam) **168**, 714 (1990)
17. For other thermodynamic theories of grains, see: B. Bernu, F. Delyon, and R. Mazighi, Phys. Rev. E **50**, 4551 (1994); J.J.Brey, F. Moreno, and J.W. Dufty, Phys. Rev. E **54**, 445 (1996)
18. Nowak et al used such a fluctuation formula to experimentally measure the compactivity of the excited grains. See: E. R. Nowak, J. B. Knight, E. Ben-Naim, H. M. Jaeger and S. R. Nagel, Density Fluctuations in Vibrated Granular Materials, Phys. Rev. E **57**, 1971-1982 (1998).
19. Jysoo Lee, cond-mat/9606013; S. Luding, E. Clément, A. Blumen, J. Rajchenbach, and J. Duran, Phys. Rev. E. **50** R1762 (1994).
20. F. R. Ree and W. G. Hoover, J. Chem. Phys. **40**, 939 (1964).
21. N. F. Carnahan and K. E. Starling, J. Chem. Phys. **51**, 635 (1969).
22. A. Kudrolli, M. Wolpert and J. P. Gollub, Phys. Rev. Lett. **78**, 1383 (1997).
23. J. S. Olafsen and J. S. Urbach, Phys. Rev. Lett. **81**, 4369 (1998); J. Delour, A. Kudrolli, and J. Gollub, cond-matt/9901203.
24. E. Grossman, T. Zhou, and E. Ben-Naim, cond-matt/9607165.
25. P. Haff, J. Fluid. Mech. vol. 134, 401 (1983).
26. B. J. Alder, W. G. Hoover, and D. A. Young, J. Chem. Phys. **49**, No.8, 3688 (1968).
27. S. Luding, *Models and simulations of granular materials*, Ph.D thesis, Albert-Ludwigs Universität Freiburg, Germany (1994). See Fig.19.
28. For Apollonian packing, see B. Mandelbrot, "The Fractal Geometry of nature," (W. H. Freeman and Company, New York, 1982).
29. The 2D simulation results by Luding and Strauß in this book are not inconsistent with our scenario. See Fig.9 (curve IV) and Fig.10 of their paper for the formation of the "Fermi rectangle" near the bottom layer. Note that in the



paper by Luding and Strauß, a density is obtained where a disorder-order transition occurs which is notably smaller than the maximum, close packed density. For other MD simulations for dense granular gases, see also, P. Sunthar and V. Kumaran, *Phys. Rev. E.* **60**, 1951 (1999)

# Density Profiles for 100 Particles, $\Omega=4$



## Density Profile for 100 Particles, $\Omega=4$ , $\Gamma=2.0$ and $\Gamma=20.0$

